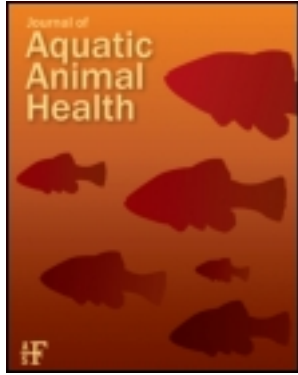


This article was downloaded by: [Jeffrey E. Smiley]

On: 13 March 2012, At: 10:19

Publisher: Taylor & Francis

Informa Ltd Registered in England and Wales Registered Number: 1072954 Registered office: Mortimer House, 37-41 Mortimer Street, London W1T 3JH, UK



Journal of Aquatic Animal Health

Publication details, including instructions for authors and subscription information:

<http://www.tandfonline.com/loi/uahh20>

Pathology of Ocular Lesions Associated with Gas Supersaturation in White Seabass

Jeffrey E. Smiley^a, Mark S. Okihiro^b, Mark A. Drawbridge^a & Ronald S. Kaufmann^c

^a Hubbs-SeaWorld Research Institute, 2595 Ingraham Street, San Diego, California, 92109, USA

^b California Department of Fish and Game, 4220 Garfield Street, Carlsbad, California, 92008, USA

^c University of San Diego, 5998 Alcalá Park, San Diego, California, 92110, USA

Available online: 12 Mar 2012

To cite this article: Jeffrey E. Smiley, Mark S. Okihiro, Mark A. Drawbridge & Ronald S. Kaufmann (2012): Pathology of Ocular Lesions Associated with Gas Supersaturation in White Seabass, *Journal of Aquatic Animal Health*, 24:1, 1-10

To link to this article: <http://dx.doi.org/10.1080/08997659.2012.668507>

PLEASE SCROLL DOWN FOR ARTICLE

Full terms and conditions of use: <http://www.tandfonline.com/page/terms-and-conditions>

This article may be used for research, teaching, and private study purposes. Any substantial or systematic reproduction, redistribution, reselling, loan, sub-licensing, systematic supply, or distribution in any form to anyone is expressly forbidden.

The publisher does not give any warranty express or implied or make any representation that the contents will be complete or accurate or up to date. The accuracy of any instructions, formulae, and drug doses should be independently verified with primary sources. The publisher shall not be liable for any loss, actions, claims, proceedings, demand, or costs or damages whatsoever or howsoever caused arising directly or indirectly in connection with or arising out of the use of this material.

ARTICLE

Pathology of Ocular Lesions Associated with Gas Supersaturation in White Seabass

Jeffrey E. Smiley*

Hubbs–SeaWorld Research Institute, 2595 Ingraham Street, San Diego, California 92109, USA

Mark S. Okihiro

California Department of Fish and Game, 4220 Garfield Street, Carlsbad, California 92008, USA

Mark A. Drawbridge

Hubbs–SeaWorld Research Institute, 2595 Ingraham Street, San Diego, California 92109, USA

Ronald S. Kaufmann

University of San Diego, 5998 Alcalá Park, San Diego, California 92110, USA

Abstract

Cultured juvenile white seabass *Atractoscion nobilis* (WSB) can suffer from intraocular emphysemas and exophthalmia in the hatchery environment. To identify the cause, two size-groups of WSB were exposed to five gas saturation levels, ranging from 98% to 122% total gas pressure (TGP), over a 96-h exposure period in 18°C and 23°C seawater. Histological examination revealed that the gross and subgross lesions associated with gas supersaturation included corneal and orbital emphysema, along with subretinal, optic nerve, and iridial hemorrhage. Corneal emphysema was the most prominent gross lesion, with the severity and prevalence increasing between size-groups and water temperatures as TGP increased. Following the same pattern was orbital emphysema, which affected more than 93% of the fish examined and caused hemorrhage in the subretinal space, around the optic nerve, in the iris, or a combination thereof. Iridial hemorrhage occurred in 91% of the fish examined and decreased significantly with fish size. The prevalence and severity of hemorrhage in the subretinal space increased significantly with TGP and fish size but not with temperature. Optic nerve hemorrhage was absent in small fish exposed at 18°C but increased significantly with temperature and fish size. The reverse was true for the large fish.

Since the 1900s, fish culturists have reported a variety of eye abnormalities in hatchery-reared fish, including corneal lesions, exophthalmia (bulging eyes), and cataracts (Allison 1962). Eye abnormalities have been linked to genetics, nutrition (Hughes 1985), stress (Steucke et al. 1968; Ubels and Edelhäuser 1987), kidney disease, hypoproteinemia, trauma, parasitism, and infection with lymphocystis virus (Dukes and Lawler 1975; Stroud et al. 1975).

Exophthalmia and corneal gas blisters also have been associated with an excess of dissolved gas in water (total dissolved gas supersaturation [TDGS]). Subadult rainbow trout *Oncorhynchus mykiss* exposed to a saturation level of 146.2%

total gas pressure (TGP) for 7 h exhibited corneal cloudiness, exophthalmia, corneal swelling, and corneal breakage, followed by collapse of the globe and necrosis (Hoffert and Fromm 1965). Chronic exposure of juvenile salmonid fish to supersaturated water often results in gas bubble disease (GBD). Symptoms of GBD include hemorrhagic eyes, choroid and retinal damage, exophthalmia, and rupturing of exophthalmic eye in extreme cases (Poston et al. 1973; Machado et al. 1987; Smith 1988; Krise et al. 1990).

At the Leon R Hubbard Jr. Hatchery in Carlsbad, California, white seabass *Atractoscion nobilis* (WSB) are raised to replenish the depleted wild fish stock off Southern California. These fish

*Corresponding author: jsmiley@hswri.org

Received January 28, 2011; accepted October 16, 2011

are grown to approximately 20 cm before being released into the ocean. Throughout their life cycle, hatchery fish are restricted to shallow (0.8-m) pools in recirculated water systems. In 1999, investigations were made regarding the increasing prevalence of juvenile WSB suffering from GBD (intraocular emphysema and exophthalmia). The cause of the problem was believed to result from increased TDGS in the seawater. Because affected fish were of substandard quality and would eventually perish from GBD, they were culled from the hatchery populations prior to release. In order to better understand and prevent GBD in the hatchery-reared WSB, we conducted TDGS exposure trials.

In this study, the effects of TDGS on two size-classes of WSB were examined during 96-h exposures to five levels of TGP at 18°C and 23°C. The goals of the study were to (1) induce GBD in juvenile WSB, (2) assess gross and histologic eye lesions associated with TDG at and above saturation levels in the hatchery, (3) compare and contrast TDGS lesions between two size-classes of WSB, and (4) evaluate differences in TDGS lesion type and severity in WSB exposed to different water temperatures.

METHODS

Fish selection.—A total of 1,200 juvenile white seabass were used in this study. All fish were obtained from the Leon R.

Hubbard, Jr. Hatchery owned and operated by Hubbs–SeaWorld Research Institute (HSWRI) in Carlsbad, California. Two size-classes were chosen for experimentation. Small fish were 59 ± 9 (mean \pm SD) d posthatch (dph) and weighed 3.2 ± 1.3 g. Large fish were 110 ± 10 dph and weighed 22.4 ± 6.1 g. All fish were screened for absence of eye lesions prior to the start of the experiments by visual observation during stocking of the systems.

Experimental design.—A total of 60 independent exposure trials were conducted in 50-L glass aquaria on a flow-through seawater system. Water depth in these aquariums was maintained at 0.25 m. (This system is described in detail in Smiley and Drawbridge 2008.) Fish were exposed to 98 (control), 102, 109, 116, and 122% TGP for 96 h at 18°C and 23°C (see also Table 1). For each temperature, 10 aquaria (10 fish in each tank) were used (two replicate tanks for each of the five TGP levels). For each size-class and temperature combination, three separate exposure trials were conducted.

The range of TGP selected for this experiment reflected values recorded in juvenile rearing systems during typical hatchery operations between 2000 and 2002. Total gas pressure levels were maintained by mixing supersaturated seawater with saturated seawater and monitored with a Hydrolab MiniSonde (ECO Environmental, Perth, Western Australia) every 8 h throughout

TABLE 1. Summary data for subretinal gas pockets (SRGPs), subretinal hemorrhage (SRH), optic nerve hemorrhage (ONH), and iridial hemorrhage (IH) scores. Data included for each TGP level are (1) mean area of SRGP (mm^2) for one eye; (2) mean scores between 0 and 3 of SRH, ONH, and IH; and (3) percent prevalence ((number of fish affected/number of fish examined)·100) for each lesion in small and large fish.

Exposure level (TGP,%)	Variable	18°C				23°C			
		SRGP	SRH	ONH	IH	SRGP	SRH	ONH	IH
Small fish mean scores									
98	Mean area or score	0.21	0.1	0	1.7	0.39	0.1	1	1.7
	Prevalence (%)	90	10	0	90	100	10	50	100
102	Mean area or score	0.3	0.3	0	1.8	0.34	0.2	0.2	1.2
	Prevalence (%)	100	30	0	100	100	20	10	70
109	Mean area or score	0.31	0.1	0	1.9	0.42	0.2	0.1	1.6
	Prevalence (%)	90	10	0	100	100	20	10	90
116	Mean area or score	0.29	0	0	1.7	0.56	0.6	0.7	1.8
	Prevalence (%)	95	0	0	90	100	60	40	100
122	Mean area or score	0.39	0	0	1.3	0.52	0.9	0.9	1.7
	Prevalence (%)	100	0	0	80	100	80	40	100
Large fish mean scores									
98	Mean area or score	0.47	0.2	0.13	0.5	0.9	0.7	0.6	1.7
	Prevalence (%)	85	20	13	50	80	50	40	90
102	Mean area or score	1.04	0.7	1	0.2	0.52	0.7	0.6	1.3
	Prevalence (%)	100	60	60	20	80	60	20	90
109	Mean area or score	1.03	0.5	0.7	0.9	0.46	0.5	0.5	1.5
	Prevalence (%)	85	50	30	90	65	50	30	80
116	Mean area or score	3.26	1	0.9	1	2.17	0.7	0.9	1.5
	Prevalence (%)	50	80	50	70	75	60	38	100
122	Mean area or score	2.48	1.4	0.7	0.9	8.62	0.9	0.1	1.7
	Prevalence (%)	75	100	40	60	75	60	11	90

the experiment. The temperatures selected reflect the two temperature regimes in which the white seabass have been reared at the hatchery. Fish were acclimated in their original culture pools to the target water temperature at 1.0°C/d prior to the start of experiments.

Histologic sample preparation.—At the end of each trial, fish were euthanized with a lethal dose (>100 mg/L) of tricaine methanesulfonate and necropsied. Standard length and wet mass were determined to the nearest 0.1 cm and 0.1 g, respectively. Of the 1,200 fish exposed, 200 were chosen for examination based on the severity of visible ocular lesions (10 per saturation level per temperature per size-class). Fish with the most severe corneal lesions were chosen preferentially because the study was designed to examine the morphology of the lesion and not the progression. Fish selected for assessment were fixed in 10% solution of neutral-buffered formalin in a 10:1 ratio of fixative to tissue.

Of the approximately 200 fish examined for SRGPs, 100 (five per saturation level per temperature per size-class) were selected for histology. Fish with the largest SRGPs were preferentially selected. The gas pocket was examined following the cut made anterior to the lens across the head of the fish (Figure 1). The pockets were measured to nearest 0.1 cm in large fish and 0.1 mm in small fish. If SRGPs were similar in size for a particular treatment level, then fish were selected at random.

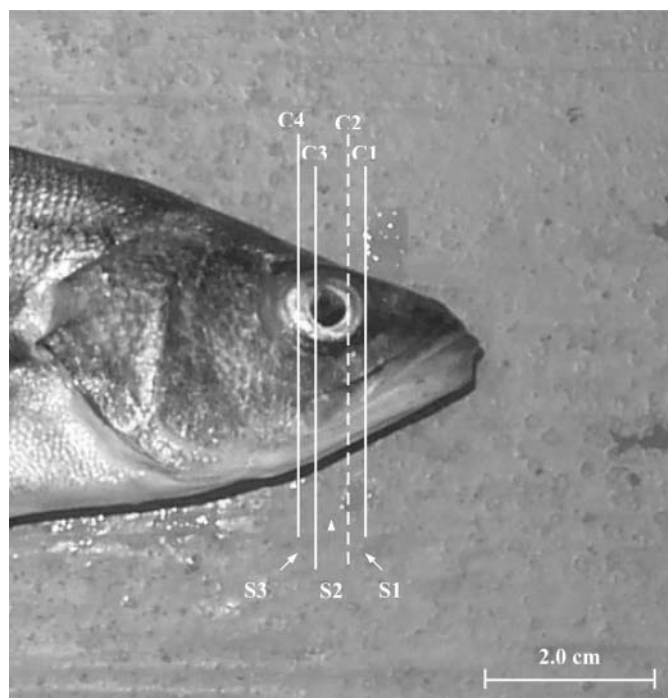


FIGURE 1. Examples of cuts made for histological evaluation of large fish eye tissues. Cuts 1 (C1) to C4 are made perpendicular to the body of the fish. Sections 1 (S1) to S3 were sent in for processing. The dashed line represents C2, where measurements were made of the internal SRGP behind the eye. The nose and body of the fish were not used for histological evaluation.

In preparation for histology, fish heads were demineralized by immersion for 24 h in Cal-Ex decalcifying solution (Fisher Scientific, Pittsburgh, Pennsylvania) at a 10:1 ratio of solution to tissue. Sections of the head, 1–2 mm thick, were made using Teflon-coated razor blades. Sections for larger fish were made anterior to the eye, anterior to the lens, posterior to the lens, and posterior to the eye (Figure 1). In smaller fish, sections were made 2–3 mm from the tip of the nose, anterior to the lens, and posterior to the lens. Demineralized fish head cross sections were submitted to the Central Histology Facility in Sacramento, California, where they were imbedded in paraffin and stained with hematoxylin and eosin.

Assessment of ocular lesions.—The surface area of the crescent-shaped SRGP was measured by making perpendicular length and width measurement of the cross-sectional cavity located anterior to the lens of the fish eye. The crescent area was then used to quantify the degree of orbital emphysema. To make these calculations, an assumption was made that the fish eye is a sphere. With the addition of a crescent-shaped gas pocket to the rear of the eye, the sphere becomes an ellipsoid, assuming the presence of a hypothetical equally sized gas pocket at the front of the eye. The creation of an ellipsoid also assumes that the eye is a relatively rigid structure and that its spherical shape does not deform following formation of the gas pocket. When making cross-sectional slices through the demineralized head and eyes, the ellipsoid is cut longitudinally and can be viewed as a two-dimensional ellipse, a circular eye section being framed by two crescents. The crescent area behind the eye is then calculated (as [area of an ellipse – area of a circle]/2).

Scoring hemorrhage intensity.—Hemorrhage was defined as a discharge or escape of blood from blood vessels. This occurred either by passage of blood cells through intact and unruptured walls (diapedesis) or by flow through ruptured walls. The intensity of hemorrhage was estimated and scored for three ocular regions: subretinal, optic nerve, and iridial. Scores for SRH were based on the percent coverage of extravasated RBCs (those not confined within intact blood vessels) between the retina and scleral cartilage. Many subretinal areas were distorted by processing artifacts or were disrupted severely following gas bubble formation behind the eye. In order to score percent hemorrhage accurately, some comparisons were made between the subretinal areas of control fish (those with relatively few artifacts) and those of the exposed fish. Criteria for ranked scores were as follows: score = 0 (not present) if there was no hemorrhage (Figure 2A); score = 1 (mild) if hemorrhage was less than 15% of the normal subretinal zone; score = 2 (moderate) if hemorrhage was 15% or greater but less than 30%; and score = 3 (severe) if hemorrhage was greater than 30% (Figure 2B).

Measurements of optic nerve and IH were made using an ocular micrometer with an Olympus CH30 compound microscope and 10× objective (total magnification = 100×). The degree of hemorrhage surrounding each optic nerve was scored semiquantitatively. Criteria for ranked scores were as follows: score = 0 (not present) if there was no hemorrhage; score = 1

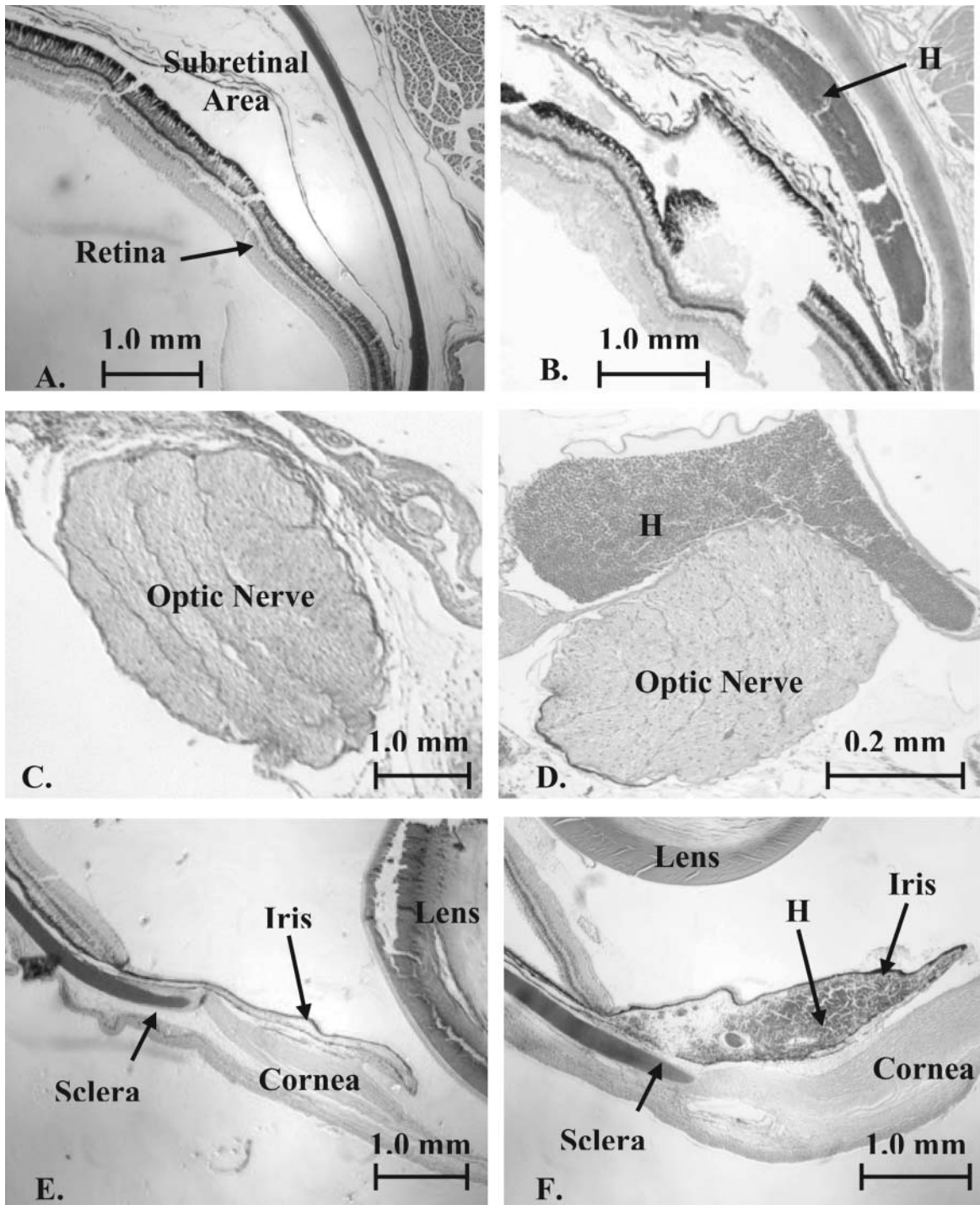


FIGURE 2. Representative examples of normal (score = 0) versus severe (score = 3) areas of hemorrhage, respectively, in the (A, B) iris, (C, D) optic nerve, and (E, F) subretinal area of the white seabass eye. Orientation is equivalent in all pairs of photos. Hemorrhage is indicated by an "H." Subretinal scores were made at the eye, while optic nerve scores were made near the base of the brain.

(mild) if the zone of hemorrhage was less than 10 cell layers thick and covered less than 25% of the optic nerve perimeter, or was less than 10 cell layers thick and less than 20 wide; score = 2 (moderate) if the area of hemorrhage was greater than 10

cell layers thick and 20 wide, or covered greater than 25% of the optic nerve perimeter; and score = 3 (severe) if the zone of hemorrhage was greater than 25% of the optic nerve area, as seen in cross section (Figure 2D).

The iris is disk-shaped with a central circular opening, the pupil. In section, the iris presented as two linear pieces of tissue (located on opposite sides of the lens); percent hemorrhage was calculated for each side. Scores for both left and right eyes were made blind, and only slide accession numbers were recorded during the scoring process. Both left and right eyes were assessed for degree of hemorrhage into the iris. The top two scores in both eyes were averaged to give a final percent hemorrhage representing a particular fish.

Percent IH was estimated visually using the entire iris. Except for very low scores (1–3%), degree of hemorrhage was estimated to the nearest 5%. One-percent hemorrhage was recorded when a single free-floating red blood cell (RBC) was observed in the iris. Three percent was used when there was more than one RBC but less than five percent of the iris was involved. Estimates of percent hemorrhage subsequently were converted to ranked scores (0–3). Criteria for ranked IH scores were as follows: score = 0 (not present) if there was 0–1% hemorrhage (Figure 2E); score = 1 (mild) if hemorrhage was greater than 1% but less than 10%; score = 2 (moderate) if hemorrhage was greater than or equal to 10% but less than 30%; and score = 3 (severe) for any iris containing 30% or greater hemorrhage (Figure 2F).

Data analysis.—Results within and among trials were compared using general linear models and Minitab Statistical Software (Minitab, State College, Pennsylvania). Initially, comparisons were run using a three-way analysis of variance (ANOVA), looking for all possible interactions (e.g., if size is independent of temperature). If no significant interactions were found, the model was run a second time without interactions. The Pearson's correlation was also used for comparison between eye lesions, saturations, and temperatures. All statistical analyses were evaluated at a 95% significance level.

RESULTS

Corneal Emphysema

Corneal emphysema (gas accumulation within the cornea) was the most prominent gross finding associated with exposure of juvenile WSB to supersaturated seawater (Smiley et al. 2011). Corneal emphysema initially manifested as discrete 1–2-mm diameter gas blisters along the outer margins of the eye (Figure 3; see also Figure 4 for comparison reference). Gross observation revealed that gas blisters were thin-walled, translucent, refractile, raised, and fixed within the cornea (e.g., they were immovable and did not migrate). While some gas blisters formed in periocular conjunctival tissue, the majority of early lesions were restricted to the cornea. Blisters appeared as early as 12 h following the onset of experimental exposure and generally progressed in size and number with exposure time. With severely affected fish, multiple blisters coalesced, forming an irregular multichambered layer covering the entire surface of the eye (Figure 3).

Prevalence and severity of corneal emphysema increased significantly with increasing TGP in both size-groups and wa-

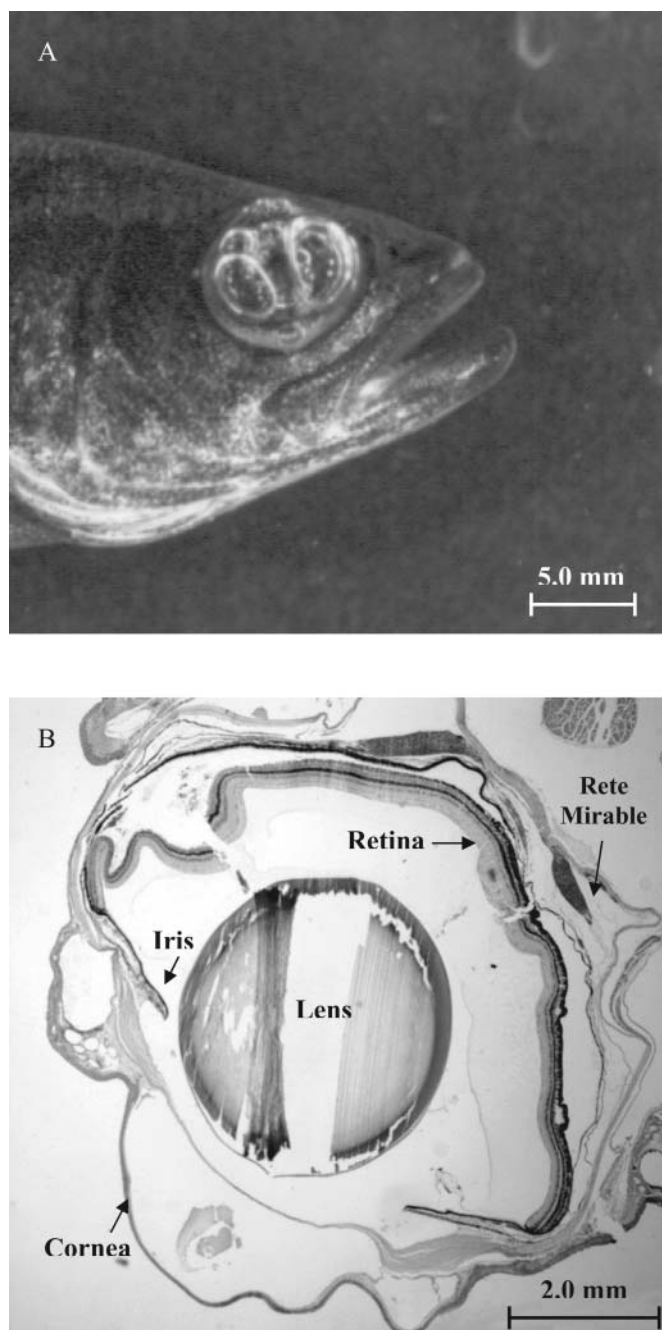


FIGURE 3. (A) Gross and (B) subgross examples of multiple gas blisters within the cornea, forming an irregular multichamber layer covering the entire surface of the eye.

ter temperatures (Smiley et al. 2011). Fish with severe corneal emphysema lost buoyancy control as lesions increased in size and occluded the eye. Eventually, affected eyes would become severely exophthalmic, bulging out of the socket and resulting in periocular hemorrhage (i.e., pop-eye). At the highest saturation level (122% TGP), corneal blisters ruptured in fish with severe emphysema, which may have partially restored vision and resolved buoyancy problems among the few fish that survived.

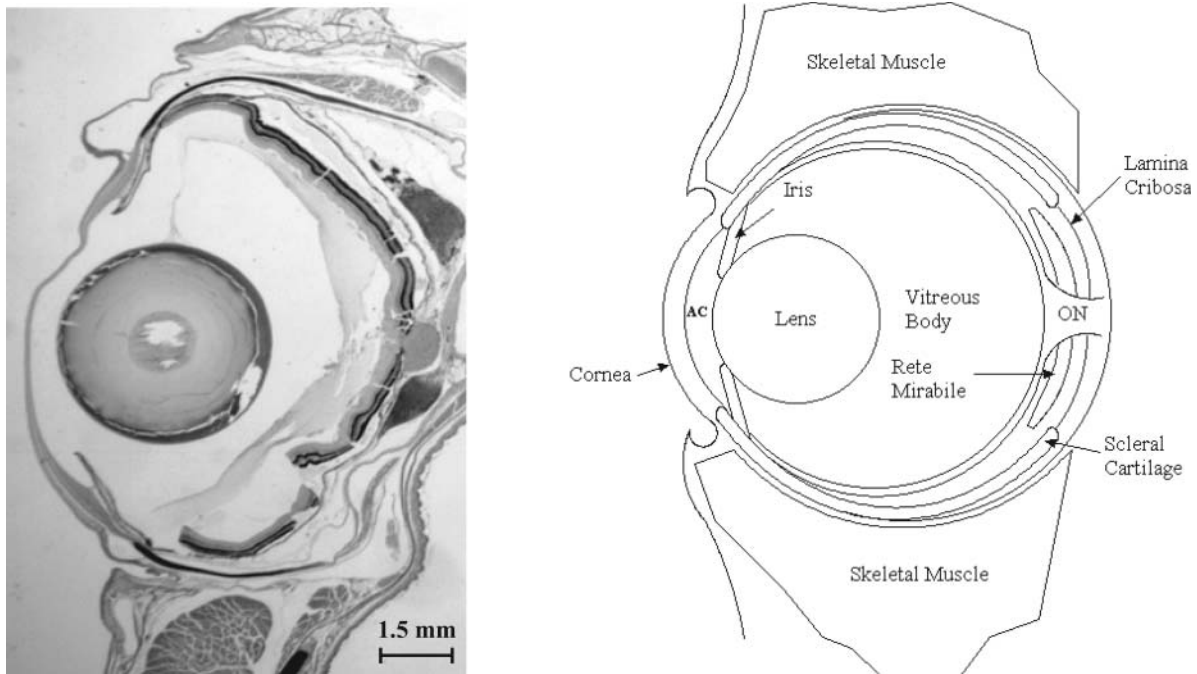


FIGURE 4. (A) Photograph of a normal white seabass eye in cross section under $20\times$ magnification. (B) Schematic of a white seabass eye in cross section. Labeled structures of interest include the lens, iris, cornea, lamina cribrosa, optic nerve (ON), anterior chamber (AC), rete mirabile, and skeletal muscle.

Histologically, corneal emphysema was characterized by dissection of the linear collagen fibers of corneal stroma (substantia propria). Affected corneas were thickened markedly, and cavities often ballooned outwards, stretching and distending the overlying epithelium and Bowman's membrane. In fish with severe emphysema (e.g., Figure 3B) corneal gas blisters were multilocular, separate cavities being separated by strands of stromal collagen. A few blisters contained small amounts of pale eosinophilic proteinaceous fluid.

Orbital Emphysema and Subretinal Gas Pocket

Orbital emphysema was characterized by marked subretinal or retrobulbar accumulation of gas (gas pockets) in both the choroid layer (between the retina and sclera) and outside the sclera (between the sclera and periocular tissues; Figure 5). In rare instances, gas was able to move within the smaller gas pockets throughout the corneal or subconjunctival tissues. Grossly, orbital emphysema presented as exophthalmia and was a common finding: 93.5% of 200 fish examined had measurable SRGPs in at least one eye and 80.5% had bilateral gas pockets. Only 6.5% had no subretinal lesions. The extent of SRGPs varied among treatments, but in severe form, the globe of the eye was prolapsed by massive gas cavities occupying up to 75% of the orbit. Large retrobulbar gas cavities usually were distributed symmetrically over the posterior of the eye, and often stretched the optic nerve as gas filled the area between the globe and socket (Figure 5B).

The severity of orbital emphysema generally increased with increasing gas saturation between small and large fish size-

classes exposed at 18°C and 23°C . The largest gas pockets (mean crescent area = 8.62 mm^2) were found among large fish exposed to 122% TGP at 23°C . Among small fish, the largest SRGPs occurred at 116% and 122% TGP at 23°C (Table 1). Comparison of orbital emphysema scores between the two size-classes revealed that mean surface area of SRGPs was consistently larger among large fish at all treatment levels.

Evaluation of prevalence data revealed that although SRGPs were larger in large fish, orbital emphysema was significantly more common among smaller fish. Prevalence of bilateral orbital emphysema among all treatment groups of small fish was either 90% or 100%. Among small fish exposed at 23°C , four of five exposure groups had 100% prevalence of bilateral lesions. In contrast, prevalence of bilateral orbital emphysema in larger fish varied from 30% to 70% among those exposed to 109–122% TGP. Of the 13 fish with no orbital emphysema, 11 were large fish, and eight of those 11 were in the three highest gas saturation groups (Table 1).

Subretinal Hemorrhage

Histologically, SRH was characterized by accumulation of blood in the choroid (ocular layer located between retina and sclera), which affected 55% of the 100 fish examined (Figure 2A, B). In severe cases, RBCs completely filled the choroid, obscuring the rete mirabile. Hemorrhaging also extended from the back of the eye toward the ciliary body (lens attachment point), blood sometimes pooling in the iris. Generally, hemorrhage increased with TDGS in three of four exposure groups (Table 1).

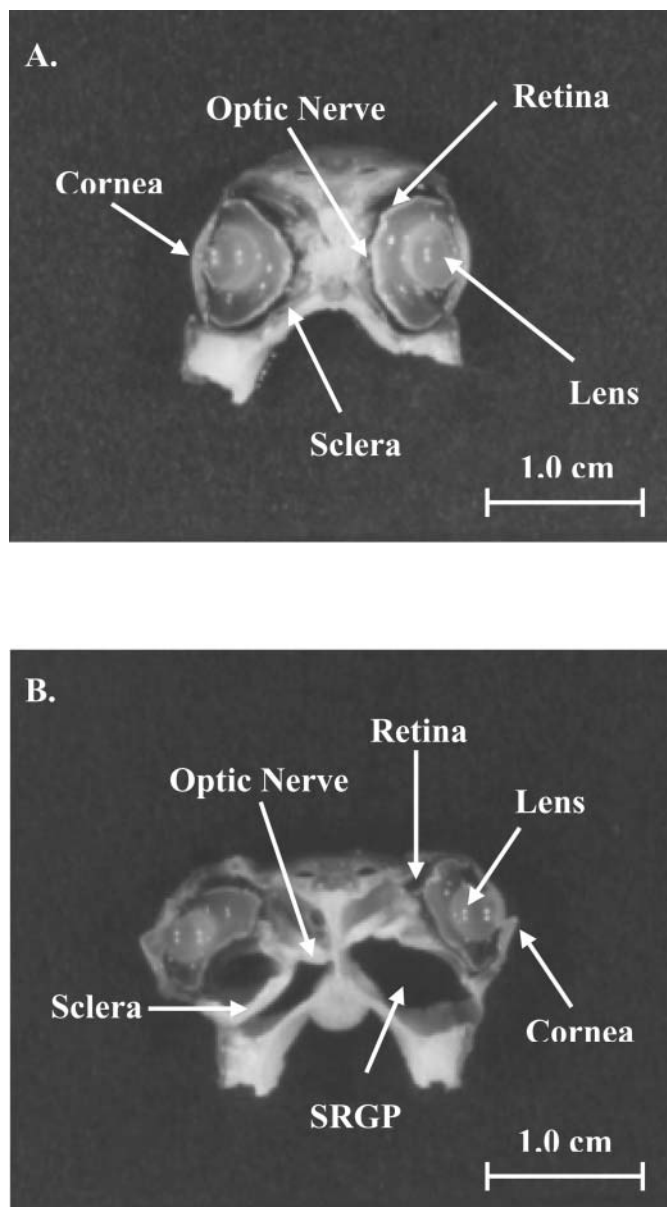


FIGURE 5. Representative cross-sectional area exposing the subretinal area in white seabass. Larger fish were chosen as representative examples because their morphology is easier to see. (A) Normal (score = 0) subretinal area of a control fish exposed to 98% TGP. (B) Severe (score = 3) SRGP in a fish exposed to 122% TGP at 23°C.

Among larger white seabass, fish exposed to TDGS in 18°C water revealed a tight correlation between hemorrhaging and gas supersaturation (Pearson's correlation: $r = 0.91$, $P = 0.03$), scores ranging from 0.2 (98% TGP) to 1.4 (122% TGP). Prevalence of SRH was also strongly correlated with TDGS ($r = 0.92$, $p = 0.028$), increasing from 20% (98% TGP) to 100% (122% TGP) prevalence. At 23°C, mean hemorrhage score (0.5–0.8) and prevalence (50–60%) changed only slightly with increasing gas saturation. Comparisons between the temperature treatments revealed that large fish in 116% and 122% TGP at 18°C had sub-

stantially more SRH compared with fish exposed in 23°C water (Table 1).

Among smaller fish, those in 18°C water had fewer and less severe SRHs compared with fish at 23°C. Overall prevalence was only 16%, and no SRHs were detected in small fish exposed to 116% or 122% TGP at 18°C. Mean scores for small fish in 18°C water did not exceed 0.3 for left and right eyes combined. In contrast, overall prevalence was 52% in small fish exposed to 23°C water, and there were strong positive correlations between TDGS and mean score and prevalence ($r = 0.94$, $P = 0.016$). Mean scores for SRH increased from 0.1 (98% TGP) to 0.9 (122% TGP), and prevalence increased from 10% to 80% in the same treatment groups (Table 1).

A three-way ANOVA revealed that SRH increased significantly with increasing TGP for small fish at 18°C and large fish at 23°C. Mean SRH score for these two groups was significantly greater at 122% TGP compared with mean scores for fish exposed at 98% and 109% TGP ($P < 0.05$). There was also a significant increase in severity of lesions with age ($P < 0.001$). Although there was a difference in mean SRH score when fish were exposed at 23°C versus 18°C, the difference was not significant ($P > 0.1$).

Optic Nerve Hemorrhage

Optic nerve hemorrhage was characterized by accumulation of RBCs along the outer perimeter of the nerve, sometimes pooling into larger aggregates along one side (Figure 2D). This was a relatively uncommon lesion: 34% of 97 fish examined had unilateral hemorrhage (cranial sections from three fish did not contain sufficient profiles of optic nerve to be assessed), 16.5% had bilateral hemorrhage, and 66% had no hemorrhage. In some fish, hemorrhage extended up to the optic chiasm and occasionally as far as the meninges lining the base of the brain.

A surprising finding was that ONH did not occur in small fish exposed in 18°C water. In contrast, 36% of small fish exposed in 23°C water had some evidence of unilateral ONH. Mean scores for hemorrhage in small fish exposed in warm water were highest among control fish exposed to 98% TGP, followed by the highest treatment group (122% TGP; Table 1).

Among large WSB, consistent patterns of ONH were difficult to find. Mean hemorrhage scores of large fish at 18°C were greater than those of fish held at 23°C for four of five treatment levels, but there was no correlation of severity with TDGS level ($r = 0.34$, $P = 0.571$). There was also no correlation among large fish held at 23°C ($r = -0.38$, $P = 0.531$), mean ONH score being highest in fish exposed to 116% TGP but lowest in fish exposed to 122% TGP.

Statistical analysis of ONH scores revealed that TGP was not a significant factor. In addition, there was a significant interaction between fish size and water temperature ($P < 0.05$). The model indicated that size-class was the only factor that significantly affected ONH scores, a significant increase in ONH occurring in larger versus smaller WSB exposed to supersaturated water ($P = 0.019$).

There was a significant increase in mean ONH score for the smaller fish held at 23°C compared with 18°C ($P < 0.001$). With larger fish, the reverse trend was true but not significant ($P = 0.138$).

Iridial Hemorrhage

Histologic assessment revealed that IH was characterized by influx of free RBCs and pale eosinophilic proteinaceous fluid into the loose connective tissue spaces of the iridial stroma. This was a common finding: 91% of 100 fish examined had measurable hemorrhage in the iris of at least one eye, 74% had bilateral hemorrhage, and only 9% had no hemorrhage. When severe, hemorrhage extended throughout the iris to the pupillary margin but it was usually distributed close to the base of the iris, near the ciliary body (attachment and control point for the lens; Figure 2F). The hemorrhage would cause the iris to swell up to 3.6 times larger than normal in small fish and up to five times larger in large fish.

Mean IH scores were inconsistent and high even in the control groups for all experiments, except large fish exposed to 18°C (Table 1). Iridial hemorrhage in this group increased in severity at higher gas saturation levels. Mean IH scores for large fish held at 23°C were consistently greater than those for the same size fish held at 18°C: 32% of large fish at 18°C had no hemorrhage in the iris, whereas 100% held at 23°C had at least unilateral IH. In general, small fish had a mean IH score that was significantly greater than that of larger fish ($P < 0.05$). In small fish held at 18°C, there was a negative correlation of hemorrhage with gas saturation ($r = -0.65$, $P = 0.232$). Mean scores were higher in the small fish exposed to 23°C at 116% and 122% TGP than for the same size fish held at 18°C, and 98% of all small fish at 23°C had at least unilateral hemorrhage in the iris.

Mean IH score for all exposed fish combined was significantly greater when fish were exposed in 23°C versus 18°C water ($P < 0.05$). Temperature effects, however, were not consistent among treatment groups. Mean IH scores for larger fish were significantly greater among fish in 23°C water, while mean IH score for smaller fish was less at 23°C ($P < 0.05$). Mean scores between size-groups were also consistently greater for small fish held at 18°C when exposed to 98, 102, and 109% TGP.

Statistical analysis revealed that an increase in TGP was not a significant factor in IH. However, there was a highly significant interaction between fish size and water temperature ($P < 0.001$). Residual plots showed equal variance, but the distribution was slightly skewed from normal at the tails.

DISCUSSION

Primary gross lesions in juvenile WSB associated with an acute 96-h exposure to water supersaturated with atmospheric air were gas emboli in fin capillaries, overinflation of the swim bladder, and eye lesions (Smiley et al. 2011). Internal subgross ocular lesions were by far the most common finding, which provided the impetus for this study. Overall, the correlation between

the severities of emphysema with warmer water was predictable (based on temperature-dependent rates of gas solubility) and is consistent with the results of several previous studies (Machado et al. 1987; Smith 1988; Krise and Herman 1991).

The Effect of Fish Size

In contrast to the relatively predictable effects of temperature on supersaturation-induced lesions, an unexpected finding was the fact that orbital emphysema was significantly more severe in larger versus smaller WSB. Small fish did have a higher prevalence of orbital emphysema, but the average SRGP size was significantly greater among larger fish than smaller in the two highest TGP treatment groups. While some differences in orbital emphysema could be attributed to baseline anatomical differences (e.g., larger eyes in larger fish and therefore an increased potential for subretinal cavities), clearly there was a predisposition for more-severe eye lesions among large fish. The primary reason why prevalence was lower among larger fish (especially those in the higher treatment groups) was probably because gas in subretinal cavities already had herniated into the cornea at the time fish were sampled.

Progression of Hemorrhagic Lesions

Of the three ocular sites where hemorrhage was assessed SRH was the most predictable, severity trends increasing with TGP. Hemorrhage was more severe in larger fish than smaller fish. In large fish, trends for IH were not as consistent, but mean scores at the two highest saturation levels were greater than those at the two lowest levels. Hemorrhage scores for smaller fish were more variable. Subretinal and ONH were common findings in smaller fish held at 23°C, but mean scores were highly variable and no consistent trends were apparent.

The sampling methods may have contributed to the greater-than-expected prevalence of hemorrhagic lesions among fish in the control and lower TGP treatment groups. Since one of the primary goals of the study was to assess histopathology of TDGS lesions, fish with the most severe lesions were selected at each stage of the evaluation process. Fish with the most severe corneal gas blisters initially were selected for formalin fixation; fish with the largest SRGPs subsequently were chosen for final histological processing. Also, fish were selected at random from hatchery stock where internal eye damage may have already been present.

Relative to the progression of lesions, hemorrhagic lesions likely occurred following emphysema from exposure to TDGS. As gas rapidly came out of solution (causing gas emboli to form), fragile capillaries in the choroid rete mirabile likely ruptured. If sequential sampling had been done, choroidal hemorrhage probably would have been detected within 24 h of exposure (certainly at the three highest TGP treatment levels and perhaps in all five) and probably would have increased in severity with time. As mentioned above, the presence of blood in the meninges as well as around the optic chiasm and nerves is evidence that blood collecting in the choroid was able to pass through breaks in the

lamina cribosa and into the orbital cavity. The amount of orbital hemorrhage was relatively small in comparison to the large volumes of gas, and there was no accompanying hemorrhage into the cornea.

Interestingly, substantial hemorrhage was detected in the irises of many WSB exposed to TDGS. Iridial hemorrhage was symmetrical in most fish and appears to have been a direct extension of choroidal hemorrhage from the rete mirabile. The most likely scenario is that blood in the choroid under high pressure from expanding gas pockets was forced in two directions: caudally along the optic nerve through the lamina cribosa into the orbit, and rostrally between the retina and sclera into the iris. It is apparent that the rostral track was the path of least resistance for the blood, as IH was a much more prominent and severe lesion than hemorrhage around the optic nerve or chiasm.

The fact that gases finally accumulated in the cornea and blood in the iris was likely due to differences in the physical properties of the two substances. Even though both gas and blood originated from the choroid rete mirabile, differences in density, viscosity, and molecular size caused them to migrate in different directions. For the expanding gas pocket, presumptive oxygen molecules (explained below) were small enough to pass relatively easily through the tightly woven collagen strands of the lamina cribosa and into the orbit. In contrast, the lamina cribosa was a substantial barrier for fluid and cellular components of blood, and the majority of blood instead was directed around the globe of the eye and pooled in the iris.

Additional support for the hypothesis that the lamina cribosa was a significant barrier to hemorrhage comes from the absence of ONH in smaller fish exposed at 18°C. The lack of ONH in any of the five treatment groups is consistent with the small size and, therefore, low pressure of SRGPs among these fish. It appears likely that in the absence of sufficient pressure and damage from herniating choroidal gas, blood cannot pass through the lamina cribosa into the orbit.

The absence of ONH in small WSB held at 18°C also may help to explain why IH scores among these fish were so high. All mean scores for IH at the three lowest TGP levels (98, 102, and 109%) were greater among small fish exposed in cold water compared with the other three TGP exposure groups (small fish exposed at 23°C and the two large fish groups). The most likely reason for this is because blood could not be shunted into the orbit (through the lamina cribosa); trapped, oxygen-rich choroidal blood instead was forced into the irises of these small fish.

For the smaller fish exposed to 18°C, all the hemorrhaged blood only had a single destination: the iris. Hemorrhaged blood in the other three exposure groups could travel in two directions: forward into the iris or back along the optic nerve. The absence of consistently higher mean subretinal and ONH scores for larger fish exposed at 23°C when compared with the same age fish exposed in 18°C water also could be partially explained by migration of blood. It was expected, especially following analysis of ocular emphysema data, that larger fish exposed in

warmer water would have more hemorrhage than those exposed in colder water. Instead, mean SRH scores were higher in larger fish exposed at 18°C for both 116% and 122% TGP, and mean ONH scores were higher in larger fish exposed at 18°C for the four highest TDGS levels. A possible explanation is that hemorrhage scores for larger fish exposed to 23°C were lowered falsely because blood penetrated to the optic chiasm or meninges of the brain, past the optic nerve, and therefore was not scored. Overall hemorrhage may have been more severe in the 23°C group if all nervous system sites (i.e., optic nerve, optic chiasm, and meninges) had been evaluated.

Experimental versus Production Culture

Another interesting discovery was that experimentally induced gas supersaturation eye lesions were distinctly different from those in fish cultured for replenishment at the HSWRI Carlsbad Hatchery. Gas supersaturation-induced eye lesions at the hatchery typically are characterized by intraocular (e.g., within the globe) accumulation of gas. In its mildest form, gas supersaturation eye lesions among fish at the hatchery are present as small gas bubbles in the anterior chamber or vitreous body. These gas bubbles are unfixed and migrate freely in the aqueous humor (our unpublished data).

In severely affected hatchery fish, the entire globe (anterior chamber, posterior chamber, and vitreous) is completely filled with gas, severely distended, and bulges out from the orbit. When the globe is filled with gas, the lens often is displaced and pushed forward, either into the anterior chamber or occasionally through the cornea. End-stage TDGS eyes are those that have ruptured and collapsed or are intact but severely infected by bacteria, fungi, or both (our unpublished data). These types of secondary infections have been reported in the eyes of sockeye salmon *O. nerka* and coho salmon *O. kisutch* when chronically exposed to TDGS as well (Stroud et al. 1975).

In contrast to intraocular accumulation of gas in hatchery-reared WSB, experimentally induced TDGS lesions were represented uniformly by orbital and corneal emphysema. The 96-h exposures conducted in this study resulted in corneal gas blisters that were fixed within stromal collagen fibers of the cornea. These fixed corneal gas blisters differed sharply from unfixed, free-floating gas bubbles of hatchery fish (those with early mild lesions) that change position within the anterior chamber if fish were rotated.

Another major difference between hatchery and experimental TDGS eye lesions was that hatchery fish develop solitary gas bubbles within the eye, while experimental fish exposed to higher gas saturation levels often had multiple gas blisters (our unpublished data). In many severely affected experimental fish, the entire cornea was covered with gas blisters of various sizes. A third difference was that no secondary bacterial or fungal infections were seen in experimentally exposed WSB.

Differences in eye emphysema pathology between hatchery and experimental WSB likely reflect differences in duration and level of exposure to supersaturated gas. While affected

hatchery-reared fish likely had been exposed chronically (weeks to months) to low-level (<105% TGP) gas saturation, the majority of experimental fish with severe lesions were exposed acutely (96 h) to high-level (110–122% TGP) gas saturation. This difference in exposure level and duration also may have been due to the differences in available water depths (0.8 m for hatchery fish and 0.25 m for experimental fish).

CONCLUSION

In summary, this study has shown that acute (96-h) exposure of juvenile WSB to conditions of gas supersaturation resulted in severe ocular hemorrhage and emphysema. Lesions originated in the choroid and migrated to different locations, depending on the severity of the insult and the nature of the extravasated material. Blood was found either to pool in the iris or to be forced retrograde along the optic nerve tract, sometimes as far as the meninges of the brain. Gas herniated through the lamina cribosa of the sclera and into the orbit before finally dissecting into the cornea. Differences in the severity of eye lesions between large and small WSB probably were due to differences in anatomy (number or length of rete capillaries), physiology (e.g., enzyme levels), or both. Differences in type of emphysematous lesions between experimental and hatchery WSB (corneal versus intraocular, respectively) are likely due to differences in severity and duration of exposure. Experimental fish in this study experienced acute high-level TDGS exposures, which appears to cause different pathology than fish exposed chronically or sporadically to low-level gas saturation in a production hatchery setting.

Because of this work, current rearing protocols in the hatchery have changed. Overall TDGS in the hatchery has been decreased with the addition of recirculating systems and large degassing towers. The thermal rearing temperatures have also been reduced to less than 20.5°C and stabilized to help with TDGS tolerance issues in the fish. These changes have effectively reduced the amount of gas supersaturated ambient water entering and circulating throughout the hatchery, along with significantly decreasing the number of fish suffering from GBD.

ACKNOWLEDGMENTS

This work was funded by the Ocean Resources Enhancement and Hatchery Program, which is administered by the California

Department of Fish and Game. We thank the entire hatchery staff for culture efforts of the fish, and we extend our gratitude to P. Yochem who provided advice on animal veterinary care and K. Gruenthal for her time spent reviewing this manuscript. All experimental procedures were also reviewed and approved by the HSWRI's Animal Care and Use Committee.

REFERENCES

- Allison, L. N. 1962. Cataracts among hatchery-reared lake trout. *Progressive Fish-Culturist* 24:155.
- Dukes, T. W., and A. R. Lawler. 1975. The ocular lesions of naturally occurring lymphocystis in fish. *Canadian Journal of Comparative Medicine* 39:406–410.
- Hoffert, J., and P. Fromm. 1965. Biomicroscopic, gross, and microscopic observations of corneal lesions in the lake trout, *Salvelinus namaycush*. *Journal of the Fisheries Research Board of Canada* 22:761–766.
- Hughes, S. G. 1985. Nutritional eye disease in salmonids: a review. *Progressive Fish-Culturist* 47:81–85.
- Krise, W. F., and R. L. Herman. 1991. Resistance of under-yearling and yearling Atlantic salmon and lake trout to supersaturation with air. *Journal of Aquatic Animal Health* 3:248–253.
- Krise, W. F., J. W. Meade, and R. A. Smith. 1990. Effect of feeding rate and gas supersaturation on survival and growth of lake trout. *Progressive Fish-Culturist* 52:45–50.
- Machado, J. P., D. L. Garling Jr., N. R. Kevern, A. L. Trapp, and T. G. Bell. 1987. Histopathology and the pathogenesis of embolism (gas bubble disease) in rainbow trout (*Salmo gairdneri*). *Canadian Journal of Fisheries and Aquatic Sciences* 44:1985–1994.
- Poston, H. A., D. L. Livingston, and D. G. Hedrick. 1973. Effect of method of introducing well water on the growth, body chemistry, and incidence of eye abnormalities of juvenile brown and rainbow trout. *Progressive Fish-Culturist* 35:187–190.
- Smiley, J. S., and M. A. Drawbridge. 2008. A simple apparatus for maintaining gas-supersaturated seawater in the laboratory for experimental purposes. *North American Journal of Aquaculture* 70:61–67.
- Smiley, J. S., M. A. Drawbridge, M. S. Okihira, and R. S. Kaufmann. 2011. Acute effects of gas supersaturation on juvenile cultured white seabass. *Transactions of the American Fisheries Society* 140:1269–1276.
- Smith, C. E. 1988. Histopathology of gas bubble disease in juvenile rainbow trout. *Progressive Fish-Culturist* 50:98–103.
- Steucke, E. W., Jr., L. H. Allison, R. G. Piper, R. Robertson, and J. T. Bowen. 1968. Effects of light and diet on the incidence of cataract in hatchery-reared lake trout. *Progressive Fish-Culturist* 30:220–226.
- Stroud, R. K., G. R. Bouck, and A. V. Nebeker. 1975. Pathology of acute and chronic exposure of salmonid fishes to supersaturated water. Pages 435–449 in W. A. Adams, editor. *Chemistry and physics of aqueous gas solutions*. The Electrochemical Society, Princeton, New Jersey.
- Ubels, J. L., and H. F. Edelhauser. 1987. Effects of corneal epithelial abrasion on corneal transparency, aqueous humor composition, and lens of fish. *Progressive Fish-Culturist* 49:219–224.